Journal of Materials Chemistry A

Accepted Manuscript

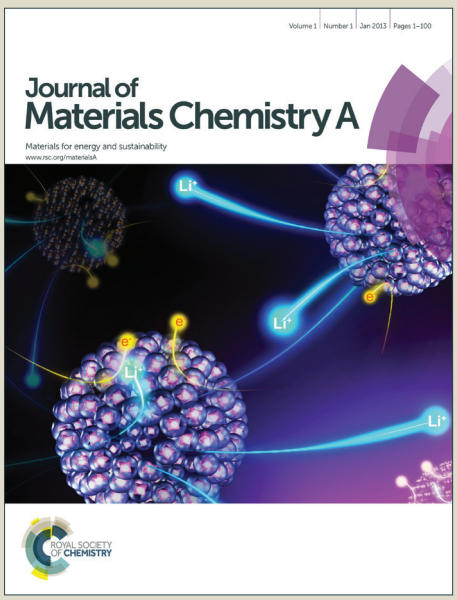

ROYAL SOCIETY OF CHEMISTRY

www.rsc.org/materialsA

Graphene supported pyrene functionalized amino-carbon nanotube: a novel hybrid architecture of Laccase immobilization as effective bioelectrocatalyst for oxygen reduction reaction

Aso Navaee [a] , Abdollah Salimi [a,b]*

[a] Department of Chemistry, University of Kurdistan, , 66177-15175, Sanandaj- Iran

[b] Research Centre for Nanotechnology, University of Kurdistan, 66177-15175, Sanandaj- Iran,

*To whom correspondence should be addressed.

Tet:+9887333624001,Fax: :+9887333624008

E-mail: absalimi@uok.ac.ir, absalimi@yahoo.com (A.Salimi)

Abstract

A facile electrochemical method to establish a 3-dimensional architecture of graphene and carbon nanotube for achieving a highly conductive platform for Laccase immobilization is described. By functionalization of the nanostructure with pyrene butyric acid using an electrochemical treatment, the efficiency of prepared nanostructure as the electrochemical platform for the oriented adsorption of Laccase is enhanced. The electrochemical analyses show that graphene enhances the bioelectrocatalytic activity of immobilized Laccase toward oxygen reduction reaction (ORR). The onset and peak potential of ORR vs. Ag/AgCl is observed at 0.64 V and 0.45 V, and peak current density is 1.92 mA cm^{-2} (when the electrode rotation speed$\rightarrow\infty$) indicating the improved biocatyalytic activity of the proposed system. The proposed methodology might give credence for the construction of a new generation of enzyme-based biocathode at mild conditions without using special chemical or reagents.

1. Introduction

Laccase (LC) is one of the multi copper oxidoreductases with many interesting possible biotechnological applications, including biosensing, biobleaching, bioremediation, chemical synthesis, wine stabilization and most importantly, biocatalytic oxygen reduction reaction under physiological conditions.[1-3] Among them ORR has been greatly considered for the designing of biocathodes in biofuel cells field. In this context, to achieve the highest biocatalytic activity, stability, selectivity and reusability, LC is commonly immobilized on solid carriers. Hence, considerable efforts have been done to establish stable and efficient immobilization techniques. The immobilization has been accomplished by different ways such as covalent binding, adsorption, entrapment, encapsulation or self-immobilization protocols and the electron can be moved by redox mediator or mediator-less (direct electron transfer, DET) between an active site of an enzyme and an electrode.[3,4] Because the additional reagent such as mediators can be harmful and may affect on the kinetics and mechanisms of electrochemical reactions, mediator-less direct electron transfer between the biocatalysts and the electrode surface are more significant.

DET of LC is achieved by favorable orientation of protein on solid surfaces. It is well known that the copper sites in the LC protein are divided into three classes: type 1 (T1) or blue copper, type 2 (T2) or normal copper, and type 3 (T3) or coupled binuclear copper centres.[5] The T1 copper center which is located close to the external surface of the protein shells, is responsible for DET of the four electrons between solid carrier (electrode) and T2/T3 centers in the enzyme substrates. Subsequently, the electrons which reached T2/T3 centers are transferred to reduce O_2 to H_2O in the solution. While, the T1center of LC is located in a hydrophobic substrate-binding pocket; so, the best approach to the suitable LC immobilization and orientation is designing the electrode surfaces with hydrophobic properties.[6]

For developing DET of LC different conductive nanoparticles, organic polymers or carbon nanomaterials have been used as interesting scaffold for enzymes immobilization.[7,8] Carbon with some unique electrical, mechanical, thermal, morphological and optical properties plays important roles in bioelectrochemistry. Among various carbon nanomaterial forms, carbon nanotubes (CNTs) which have

unique size, shape, very high specific surface area and particularly large length-to-diameter ratio,[9] are more biocompatible and accessible to both electrochemistry and immobilization of biomolecules.[10] Hence, CNTs have attracted more attention for oxidase enzymes immobilization,[11,12] and the biocatalytic applications of these enzymes in biofuel cells development. To enhance the interaction efficiency, the chemical modifications of the surface or ends of CNTs might be used where, modulate the tethering of the nanotube with other nanotubes, holder surface, solvent or nanomaterials and biomolecules.[13] Therefore, it is expected that the efficiency of CNTs toward tethering of LC can be further improved through surface functionalization, particularly, using nonpolar compounds to achieve hydrophobic scaffold.[5,6,14-16] Due to the outstanding chemical properties of amino-containing materials, the amino-substitute CNT is expected to enhance the functionalization efficiency compared to pristine CNT where, exhibited promising tendency to binding polymers and biological systems.[17,18]

Graphene (Gr) as a two dimensional structure and another interesting form of sp^2 hybridized carbon-based nanomaterials, exhibits a variety of remarkable properties including high electron mobility at room temperature, exceptional thermal conductivity and remarkable mechanical properties.[19] These properties supplemented with high specific surface area and high tendency to physical and chemical interactions to another Gr sheets or other materials, make Gr as a superior substrate to support nanomaterials in energy conversion and other related technologies.[19,20] So, the two-dimensional carbon supported CNT takes unique advantages of both ingredients and is likely to become a talented three-dimensional (3D) architectures for various applications,[21] particularly, designing bioelectrodes.[22,23] Here, we accumulate amino-CNTs on Gr nanosheets (GrNSs) to establish a 3D structure to enhance the electron transfer flux. The resulting amino-CNTs-Gr is functionalized with pyrene butyric acid (PBA) for substantial LC immobilization and performed for electrocatalytic ORR.

2. Experimental section

2.1. Materials and instruments

NH_2 functionalized Multi-Walled Carbon Nanotubes (Ref. MWCNTNH$_2$), -NH_2 functionalization is aprox. 0.5%, measured by XPS, with purity of 95%, surface specific area of 480 m^2 g^{-1}, a diameter of 20-30 nm and 1 μm length were obtained from DropSens (Spain). Laccase (LC) from Trametes Versicolor (EC Number 420-150-4) and PBA were prepared from Sigma Aldrich. Graphene oxide and its reduced form was synthesized based on the hummers method (supporting information). All electrochemical experiments were performed using an AUTOLAB modular electrochemical system (ECO Chemie, Ultrecht, The Netherlands) equipped with a PGSTAT 101 module and driven by GPES (ECO Chemie) in conjunction with a conventional three electrodes system. A glassy carbon (GC) electrode (A= 0.0314cm^2) was employed as the working electrode and a platinum wire and Ag/AgCl/ 3 M KCl as the counter electrode and the reference electrode, respectively. Scanning electron microscopy (SEM) images were obtained with a MIRA3 TESCAN HV: 20.0 KV. FTIR spectra of KBr discs containing 0.1 mg of prepared amino-CNTs before and after electrochemical conditioning were obtained by a Vector-22 BRUKER spectrophotometer. The Z View software was used for fitting the impedance data.

2.2. Preparation of the modified electrodes

At first, the 2.0 mm GC disk electrode was polished with a 0.05 μm alumina slurry and washed with water, then 5 μL of 1 mg mL^{-1} of GrNSs which dispersed in N,N-dimethylformamide/ DMF, was cast on the electrode surface. After drying in oven ~40 ^oC, the Gr-based electrode was pretreated in PBS solution pH~10 at the potential range of 0.0 to +1.6 V vs Ag/AgCl using 20 successive potential cycling. After that, 5 μL of 1 mg mL^{-1} of amino-CNTs (dispersed in DMF) was cast on the resulting Gr-based electrode and then dried in oven ~40 ^oC. The functionalization of amino-CNTs were performed using an electrochemical conditioning at the potential range of 0.0 to 1.4 V in the 1:1 acetonitrile/DMF solution containing 1 mM of PBA and 0.05 M tetraethyl ammonium hexafluorophosphate as supporting

electrolyte. The immobilization of LC on target PBA-amino-CNTs-Gr modified electrode and two other types of electrodes including pristine amino-CNT-based electrode with or without PBA functionalized, was performed by casting 10 μL of 0.3 mg mL^{-1} LC (which was dissolved in 0.1 M PBS), pH=5, overnight.

3. Results and discussion

The electrode surface modification procedure was carried out as shown in Scheme 1. In the first step Gr is assembled on the surface of glassy carbon electrode (GCE) followed by electrochemical pretreatment during 20 successive potential cycling in PBS solution with pH~10 in the potential range of 0.0 to +1.6 V vs Ag/AgCl. In general the electrochemical conditioning leads to creation hydroxyl functional groups on carbon materials,[24] that in our case, on the edge of GrNSs. The stacked GrNSs in this method gain highly stability via interaction of hydroxyl functional groups with electrode surface whereas other sides can be provided for contribution to the next possible interactions. For investigation the effect of electrochemical condition on the electrochemical properties of GC electrode modified with graphene, cyclic voltammograms of GC and GC/Gr modified electrode in aqueous solution containing of 1 mM of K_3FeCN_6/K_4FeCN_6 and 0.1M KC1 was recorded (not shown). The obtained results indicate for pretreated GC/Gr modified electrode the ΔE (E_{pa}-E_{pc}) decreased while an increase in current density is observed. Hence, during electrochemical pretreatment of GCE/Gr modified electrode hydroxyl functional groups created, both the surface area and electron transfer kinetics are increased. It has been demonstrated that the sp^2/sp^3 hybrid structure which is located on the edge moieties of carbon-based materials, exhibits the highest reactivity and electron transfer activity in contact to other materials.[25,26] Therefore, the inside-out of Gr on the electrode surface shares the aforementioned hydroxyl groups to hold amino-CNT and facilitates the electron transfer.

Here Scheme 1

As mentioned in the experimental section, the accumulation of amino-CNTs on Gr was done by casting 5 μL of dispersed amino-CNTs (1 mg mL^{-1} in DMF) on the resulting Gr/GCE. After drying in vacuum, the amino-CNTs-Gr were formed on the surface of electrode and could be well stabilized by hydrogen bonding between hydroxyl groups of Gr and amino groups of CNTs. Designing hydrophobic surface was performed using an electrochemical procedure in the presence of PBA. To this end, the amino-CNTs-Gr-based electrode was inserted in the acetonitrile/DMF solution containing 1 mM of PBA and 0.05 M tetraethyl ammonium hexafluorophosphate as supporting electrolyte. The potential cycling was applied at 0.0 to 1.4 V vs Ag/AgCl during 10 interval cycles. Based on the obtained results and the previous reported ones for oxidation of polycyclic aromatic compounds, [27] the upper limit potential of +1.4 V is enough high to oxidize the benzyl moieties of PBA to benzyl radical cations according to following equation:

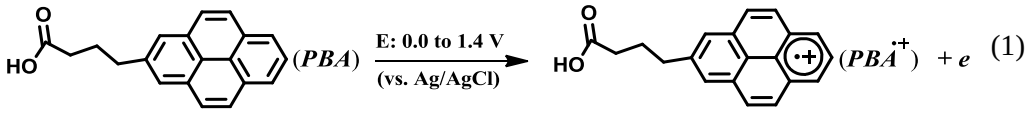

(1)

The resulting benzyl radicals are reactive enough for the nucleophilic attack by closest amino groups.[28] Herein, amino-CNTs at the electrode surface react with PBA radical according to following reactions:

$$PBA^{\bullet+} + H_2N\text{-}CNT \rightarrow PBA\text{-}HN\text{-}CNT + H^+ + e^- \quad (2)$$

$$nPBA^{\bullet+} + PBA\text{-}HN\text{-}CNT \rightarrow (PBA)_n\text{-}HN\text{-}CNT + H^+ + ne^- \quad (3)$$

Here Figure 1

Figure 1A represents the obtained cyclic voltammogram of amino-CNTs-Gr-based electrode in acetonitrile solution in the absence (a) and presence (b) of PBA. As illustrated in the presence of PBA at the forward scan, a well-defined response with a peak potential of 1.2 V is observed due to the oxidation of benzyl moieties of PBA.[27] In the reverse scan, two distinct reduction peaks at E_{pc}= 0.75V and E_{pc}=

0.35V appeared, whereas, in the solution free of PBA, almost a smooth line can be observed without any recognizable redox peak, indicating the oxidation of PBA during the electrochemical procedures. Figure 1B shows the obtained cyclic voltammograms (CVs) using modified electrode in the presence of PBA during 10 repeated cycles. As can be seen, two pairs of redox peaks at Ep_{a1}= 0.45V, Ep_{c1}= 0.35V and Ep_{a2}= 0.8, Ep_{c2} = 0.75 appeared in the second scan and grew up continually with the increase of the cycle numbers. After 10 sequence cycles, the observed peak at 1.2 V practically diminished and the derived redox peaks consistently remained. Furthermore, as can be seen in Fig.1B during potential cycling the peak potential shifted to positive values, due to formation of electropolymerized film of PBA on the carbon nanotubes surface and decreasing of surface conductivity. These peaks may likely attributed to the redox amino-bridges which formed between NH_2-CNTs and PBA molecules (PBA-NH-CNT) during the oxidation of PBA followed by the chemical reactions with NH_2 moieties of CNTs or electropolymerization of PBA on amino-CNT and formation of $(PBA)_n$-HN-CNT, respectively. When the electrode was rinsed with acetonitrile and then the CV scanned at the same potential window (0.0 to 1.4 V) in 1:1 acetonitrile/DMF solution, the same redox peaks was observed again. This clearly demonstrates the fact that the amino-CNTs well functionalized with PBA during potential cycling (Figure 1C). This configuration makes CNTs/PBA as a convenient hydrophobic substrate to attract the hydrophobic pocket of LC, as a consequence, it facilitates the direct electron transfer from LC to the electrode.

The comparison of FTIR spectra of amino-CNTs after (a) and before (b) the electrochemical conditioning implies some changes in the chemical nature of amino-CNTs caused by electrochemical cycling in the solution containing PBA (Figure 1D). Both resources display intense peaks in the region of 3406-3520 cm^{-1} attributed to N-H stretching and in 2850-2920 cm^{-1} attributed to C-H stretching. The peaks at 1614 cm^{-1} are attributed to C=C stretching and at 1374 cm^{-1} arise from C-H bending. As can be seen, the intensity of N-H stretching peaks decreases after electrochemical procedure, whereas the intensity of peaks related to C-H stretching and bending increase because of attending C-H group of PBA in the IR absorption. Moreover, another outstanding difference in IR spectra is the appearance of a peak at

1716 cm^{-1} attributed to C=O stretching for PBA-amino-CNTs-Gr compared to amino-CNTs-Gr, which can arise from carboxyl group of PBA. These results clearly identify the attachment of PBA to the surface of amino-CNTs.

Figure 2 represents the scanning electron microscopy (SEM) images of pretreated GrNSs/GC (A), assembled amino-CNTs on GrNSs/GC electrode (B) and amino-CNTs-GrNSs/GC electrode after potential cycling in the solution containing PBA (C). As can be seen, the GrNSs well stabilized on the GC surface and tethered to the electrode surface via their edge moieties. After assembling the amino-CNTs, the uniform layers of CNTs cover inside-out of the GrNSs on the electrode surface with the lowest agglomeration. Moreover, the accumulated CNTs before electrochemical pretreatment in the solution containing PBA look like baggy hair, whereas after treatment by PBA they stick together as a result of PBA attachment. The outcomes indicate that a conjugated structure is formed between the amino-CNT and Gr with highly effective surface area and superficial hydrophobic functional groups as an appropriate substrate for physical adsorption of LC.

To further investigate the changes in the surface properties, the charge transfer resistance of the modified electrode during stepwise construction was measured, using electrochemical impedance spectroscopy (EIS). The recorded Nyquist plots of the modified electrodes during stepwise construction in 1 mM K_3FeCN_6 /K_4FeCN_6 and 0.1 M KC1 aqueous solution at a polarization potential of 0.3 V vs. Ag/AgCl and the frequency range of 10 mHz to 100 KHz are shown in Figure 3. The impedance data were fitted to Randle's equivalent circuit model (Figure 3, inset) and the results are given in Table 1. R_s in the equivalent circuit is the electrolyte resistance, R_{ct} is the charge-transfer resistance, W_o is the Warburg element represents the impedance of semi-infinite diffusion of ions into the electrode in the lower frequency region and *CPE* is the constant phase element representing the double-layer capacitance. As shown in Table 1, during the modification of GCE by GrNSs and amino-CNTs, R_{ct} is significantly decreased from 17.23 to 4.01 and 0.01 KΩ for Gr and amino-CNTs-Gr modified GCE, respectively. These results indicate the small value of charge transfer resistance of Gr and CNT modified GCE and the high conductivity of amino-CNTs-Gr conjugated structure. Upon electrochemical attachment of the PBA

to the CNT surface, R_{ct} slightly increases up to 0.47 KΩ suggesting the superficial hydrophobic functional groups on the amino-CNTs-Gr-based electrode, which is appropriate scaffold for the physical adsorption of LC. Subsequently, LC immobilization on the PBA-amino-CNTs-Gr considerably hinders the charge transfer as R_{ct} reached 166.42 KΩ. Furthermore, during stepwise fabrication of the modified electrode, W_o and *CPE* considerably have changed. W_o significantly decreases from 44.85 kΩ cm^{-2} for GC to ~0.0 for LC/amino-CNTs-Gr/GC. Whereas, during the modification processes, *CPE* value increases from 0.67 to 280.62 μF $s^{\alpha-1}$. Because the Warburg impedance is only valid when the diffusion layer has an infinite thickness,[29] the results signify the fact that the double-layer diffusion decreases during the stepwise accumulation of modified layers on the electrode. Therefore, after LC immobilization the charge-transfer resistance impacts the electrochemical processes. The EIS analysis clearly demonstrated the existence and the effects of each material on the electrode resistance.

Here Figure 3

Here Table 1

The immobilization of LC on PBA-amino-CNTs-Gr modified electrode was performed by casting 10 μL of LC solution (0.3 mg mL^{-1} in 0.1 M PBS, pH=5), overnight. Also, LC was immobilized on two other electrodes, pristine amino-CNT-based electrode with and without PBA functionalization in order to comparison with target electrode. The electrocatalytic properties of the modified bioelectrodes toward ORR were tested using cyclic voltammetry technique under nitrogen and oxygen saturation conditions in 0.1 M PBS solution, pH 5, with the scan rate of 10 mV s^{-1}. Figure 4 represents the electrocatalytic activity of immobilized LC on pristine amino-CNTs (A), PBA functionalized amino-CNT (B) and PBA functionalized amino-CNT-Gr (C), for oxygen reduction reaction. As shown, all bioelectrodes display a clear CV peak related to direct O_2 reduction. The onset potential of LC/PBA-amino-CNT-Gr is about 0.64 V vs Ag/AgCl and a limiting plateau is reached at 0.45 V, showing 0.06 and 0.03 V lower over potentials compared to state (A) and (B), respectively. Furthermore, the PBA-amino-CNTs modified electrode exhibited a 3-fold increase in the current density compared to pristine amino-CNTs. When

graphene is used as a support for the PBA-amino-CNTs, the biocatalytic current density increased to 0.8 mA cm^{-2}, providing 5.4 and 1.8 fold enhancement compared to pristine amino-CNTs and PBA-amino-CNTs, respectively. To the best of our knowledge, the current density of the proposed bioelectrode for ORR is higher or comparable to reported values for all other LC based modified electrodes (Table S1). These results point to the fact that functionalization of amino-CNTs with PBA yields hydrophobic substrate that the T1 site of LC can be closed to the electrode surface for the offering DET. In the meantime, the GNSs with high conductivity provide a large surface area to suitable stacking the amino-CNTs and enhancement in the electrocatalytic response of the enzyme by electron tunneling.

Here Figure 4

Also the rotating disc electrode (RDE) voltammetry technique was performed to investigate the holding efficiency of amino-CNTs-Gr-based electrode for LC enzyme. Catalytic capability and the resulting Koutecky-Levich plots are shown in Figure S1. As shown in Figure 4D, with increasing of the rotation rate, the current density increases as a result of enhancement in mass transfer of O_2 to the electrode. As can be seen, the current density for a motionless condition at the plateau region is about 0.8 mA cm^{-2}, while increasing the rotation rate up to 2000 rpm increases the current density consecutively up to -1.4 mA cm^{-2}. Moreover, the onset and plateau reaching potential is equal to the one of motionless condition as mentioned above. These results illustrate that LC retained on the electrode surface and the kinetic of DET is rather fast. Furthermore, the electron transfer from electrode to the LC can be accelerated by amino-CNTs-Gr architecture.

To evaluate the kinetic parameters related to electrocatalytic activity of immobilized LC for the ORR including transfer coefficient (α), the rate of electron transfer at the electrode (k_{et}) and standard heterogeneous electron transfer rate constant (k_s) of all three electrodes, the Tafel plots were drawn (Figure 5). By analyzing the slopes and intercepts of linear curves obtained from log J vs. overpotential

(η) at the kinetic-control region the kinetic parameters were calculated using the following equations (3, 4, 5)[30] and the results are given in Table 2:

$$J_o = nF\, k_{et} C \qquad (3)$$

$$slop = \frac{-\alpha nF}{2.3RT} \qquad (4)$$

$$E_p = E^{\circ\prime} - \frac{RT}{\alpha nF}\left[0.780 + \ln\left(\frac{D^{\frac{1}{2}}}{k_s}\right) + \ln\left(\frac{\alpha nF\nu}{RT}\right)^{\frac{1}{2}}\right] \qquad (5)$$

where, $E^{\circ\prime}$ is the standard electrode potential (0.67 V vs. Ag/AgCl),[22] D is the diffusion coefficient of O_2 (1.9×10^{-5} cm^2 s^{-1}), ν is the scan rate (10 mVs^{-1}), J_o is the exchange current density equal to Tafel intercept and C^* is the bulk concentration of O_2 (1.25×10^{-6} $molcm^{-3}$). In addition, n, F, R and T are the number of electron transferred, Faraday constant, gas constant and ambient temperature, respectively.

Here Figure 5

Here Table 2

Taking into account the 4-electron reduction of O_2 on the all three electrodes, from the Tafel intercept and using equation 3, the amounts of k_{et} can be calculated. Moreover, the values of α can be computed from the Tafel slope using equation 4. By inserting the α values into equation 5 which have been given for totally irreversible systems,[22,30] the amounts of k_s can be achieved. The comparison the data presented in Table 1 reveal that after the functionalization of amino-CNTs with PBA, the exchange current density and electron transfer rate dramatically increase by several orders of magnitude, suggesting that PBA properly orients the LC on the electrode surface which facilitates the DET. As expected, employing the GNSs as a substrate for amino-CNTs enhances the J_o and k_{et} twice, indicating that Gr improves the electron transport between the enzyme and the electrode. The comparison of the peak potential of O_2 reduction (E_p) and transfer coefficient (α) also support the argument which discussed above. Thereupon, the PBA functional groups on the amino-CNTs adsorbs the LC in a proper way and CNT-Gr architecture

acts as a good conductive material enhances the electrocatalytic response of the enzyme. The comparison of k_s values of amino-CNTs and PBA-amino-CNTs does not show significant differences. While, presence of Gr on the electrode surface enhances the k_s value almost by 3.3 orders of magnitude compared to the conditions that Gr have not been used. These results show that the CNT and Gr as high conductive materials play a significant role in decreasing the potential energy barrier value for the O_2 reduction and also show that PBA alters the orientation of enzyme and holds it appropriately on the electrode.

The catalytic activity of LC/PBA-amino-CNTs-Gr modified electrode was examined at three different pHs close to the physiological pH value (5.0, 6.0 and 7.0). As it can be seen in Figure S2, at all pH solutions, the modified electrode shows the biocatalytic activity toward ORR (see supporting information). Furthermore, the modified electrode exhibits proper stability over a long period and the depletion in the current density was about 7% after 4 days. Also, after ~4 hours of continues application of the LC-based electrode, no depletion in the current density was seen (Figure S3), which indicated good stability of the LC-based modified electrode.

4. Conclusions

In this work, we prepared the amino-carbon nanotubes conjugated graphene nanosheets followed by PBA functionalization via an electrochemical procedure to design a hydrophobic substrate for the oriented immobilization of LC. The resulting bioelectrode showed high electrocatalytic activity toward ORR at a lower overpotentials with higher stability and improved current density. The kinetic and EIS analysis revealed the roles of the materials (PBA, amino-CNTs and Gr) which were used in the bioelectrode design. The observed results also indicated the high potential application of CNT-Gr architecture as highly conductive nanomaterials in different bioelectrochemistry fields including bioelectrode fabrication, biofuel cell design and the construction of various bioelectronics devices.

Acknowledgments: This research was supported by the Iranian Nanotechnology Initiative and the Research Office of the University of Kurdistan.

Available supporting information: Materials and Method, graphene synthesis, Table S1, pH and stability study of the modified electrode.

References

1 S.R. Couto and J.L.T. Herrera, *Biotechnol. Adv*. 2006, **24**, 500-513.

2 P. Giardina, V. Faraco, C. Pezzella, A. Piscitelli, S. Vanhulle and G. Sannia, *Cell. Mol. Life Sci*. 2010, **67**, 369-385.

3 M.F. Fernández, M.A. Sanromán and D. Moldes, *Biotechnol. Adv.* 2013, **31**, 1808-1825 and reference therein.

4 R.F. Taylor, *Protein Immobilization: Fundamentals and Applications*, Marcel Dekker, Inc., New York, **1991**.

5 S. Shleev, J. Tkac, A. Christenson, T. Ruzgas, A.I. Yaropolov, J.W. Whittaker and L. Gorton, *Biosens. Bioelectron*. 2005, **20**, 2517-2554.

6 M.S. Thorum, C.A. Anderson, J.J. Hatch, A.S. Campbell, N.M. Marshall, S.C. Zimmerman, Y. Lu and A.A. Gewirth, *J. Phys. Chem. Lett*. 2010, **1**, 2251-2254.

7 S. Shleev, A.J. Wilkolazka, A. Khalunina, O. Morozova, A. Yaropolov, T. Ruzgasd and L. Gorton, *Bioelectrochemistry* 2005, **67**, 115 - 124.

8 D. Selloum, A.A. Chaaya, M. Bechelany, V. Rouessac, P. Mielea and S. Tingry, *J. Mater. Chem. A* 2014, **2**, 2794-2800.

9 H. Dai, *Acc. Chem. Res.* 2002, **35**, 1035-1044.

10 R. Klingeler and R.B. Sim (Eds.), *Carbon Nanotubes for Biomedical Applications, Carbon Nanostructures*, Springer-Verlag Berlin Heidelberg **2011**, 97-123.

11 W. Zheng, H.M. Zhou, Y.F. Zheng and N. Wang, *Chem. Phys. Lett*. **2008**, *457*, 381-385.

12 M. Falk, Z. Blum, S. Shleev, *Electrochim. Acta* 2012, **82**, 191–202.

13 Y.P. Sun, K. Fu, Y. Lin, W. Huang, *Acc. Chem. Res*. 2002, **35**, 1096-1104.

14 M. Bourourou, K. Elouarzaki, N. Lalaoui, C. Agnes, A.L. Goff, M. Holzinger, A. Maaref and S. Cosnier, *Chem. Eur. J*. 2013, **19**, 9371-9375.

15 N. Lalaoui, K. Elouarzaki, A. Le Goff, M. Holzinger and S. Cosnier, *Chem. Commun*. 2013, **49**, 9281-9283.

16 F. Giroud and S.D. Minteer, *Electrochem. Commun.* 2013, **34**, 157–160.

17 K. Awasthi1, D. P. Singh, S. K. Singh, D. Dash and O.N. Srivastava, *New Carbon Mater*. 2009, **24**, 301-306.

18 T. Ramanathan, F.T. Fisher, R.S. Ruoff, L.C. Brinson, *Chem. Mater*. 2005, **17**, 1290-1295.

19 D. Jiang and Z. Chen (Eds), *Graphene Chemistry: Theoretical Perspectives*. John Willy and Sons Ltd. **2013**.

20 V. Georgakilas, M. Otyepka, A.B. Bourlinos, V. Chandra, N. Kim, K.C. Kemp, P. Hobza, R. Zboril and K.S. Kim *Chem. Rev.*, 2012, **112**, 6156–6214.

21 S. Nardecchia, D. Carriazo, M.L. Ferrer, M.C. Gutierrez and F. del Monte, *Chem. Soc. Rev.* 2013, **42**, 794−830.

22 Y. Umasankar, D.B. Brooks, B. Brown, Z. Zhou and R.P. Ramasamy, *Adv. Energy Mater.* 2014, **4**, DOI: 10.1002/aenm.201301306.

23 K.P. Prasad, Y. Chen, P. Chen, *ACS Appl. Mater. Interfaces* **2014**, *6*, 3387−3393.

24 J.G. Roberts, B.P. Moody, G.S. McCarty and L.A. Sombers, *Langmuir*, 2010, **26**, 9116–9122.

25 S. Hirono, S. Umemura, M. Tomita and R. Kaneko, *Appl. Phys. Lett.*, 2002, **80**, 425-427.

26 D. Kato, N. Sekioka, A. Ueda, R. Kurita, S. Hirono, K. Suzuki and O. Niwa, *J. Am. Chem. Soc*., 2008, **130**, 3716-3718.

27 F.E. Beideman and D.M. Hercules, *J. Phys. Chem*. 1979, **83**, 2203-2209.

28 M.S. Workentin, L.J. Johnston, D.D.M. Wayner and V.D. Parker, *J. Am. Chem. Soc*. 1994,**116**, 8279-8287.

29 X.Z. Yuan, C. Song, H. Wang and J. Zhang, *Electrochemical Impedance Spectroscopy in PEM Fuel Cells: Fundamentals and applications*, Springer-Verlag London Limited, **2010**.

30 A.J. Bard and L.R. Faulkner *Electrochemical methods. Fundamentals and applications* (2^{th} ed.), Wiley, **2001**.

Scheme, figures and tables caption

Table 1: Impedance fitting parameters of different modified electrodes.

Table 2: Comparison of electrochemical and kinetic parameters of direct O_2 reduction by LC modified different electrodes.

Scheme 1: The preparation procedures of LC/amino-CNTs-Gr-based electrode.

Figure 1: (A) Recorded CVs with scan rate of 0.1 V s^{-1} from the amino-CNTs-Gr-based electrode in the 1:1 acetonitrile/DMF solution containing 1 mM of PBA and 0.05 M tetraethyl ammonium hexafluorophosphate as supporting electrolyte, in the absence (a) and presence (b) of PBA. (B) Recorded cyclic voltammograms of GC/Gr/NH2-CNTs modified electrode in acetonitrile/DMF solution containing 1 mM of PBA and 0.05 M tetraethyl ammonium hexafluorophosphate during 6 interval cycles. (C) Recorded CV of GC/Gr/NH2-CNTs/PBA modified electrode in 1:1 acetonitrile/DMF solution containing 0.05 M tetraethyl ammonium hexafluorophosphate. (C) FTIR spectra of amino-CNTs after electrochemical pretreatment in solution containing PBA (a) and pristine amino-CNTs (b).

Figure 2: A) SEM image of GrNSs after electrochemical pretreatment at GCE. B and C represent the SEM image of amino-CNT on Gr-based electrode before and after electrochemical conditioning in PBA solution, respectively.

Figure 3: The electrochemical impedance spectra of GCE (a), Gr/GCE (b), amino-CNTs-Gr/GCE (c), PBA-amino-CNTs-Gr/GCE (d) and after LC treatment (e). Inset represents the equivalent circuit fitting.

Figure 4: Recorded CVs at 0.1 M PBS, pH=5, scan rate=10 mV s^{-1} attributed to immobilized LC on pristine amino-CNT (A), amino-CNT (B) and amino-CNT-Gr (C) after electrochemical conditioning in presence of 1 mM of PBA and 0.05M tetraethyl ammonium hexafluorophosphate as supporting electrolyte, under N_2-suturated (dotted line) and O_2 saturated (smoothed line). D) Recorded LSVs using a rotating disc electrode at different rotation rate (0, 500, 1000, 1500, 2000 rpm from top to down).

Figure 5: Tafel plot of immobilized LC on amino-CNTs (a), PBA-amino-CNTs (b) and PBA-amino-CNTs-Gr (c) modified GCE.

Table 1: Impedance fitting parameters of different modified electrodes.

Element	a) GCE	b) (a) + Gr	c) (b) + amino-CNTs	d) (c) + PBA	e) (d) + LC
R_{ct} (kΩ)	17.24	4.01	0.01	0.47	166.42
W_o-R (kΩ)	44.85	45.80	0.26	3.70	0.00
CPE-T (μF $s^{\alpha-1}$)	0.67	3.90	260	6.50	280.62

Table 2: Comparison of electrochemical and kinetic parameters of direct O_2 reduction by LC modified different electrode.

Electrode	E_p / V	T. slope / dec.V^{-1}	J_o / A cm^{-2}	α	k_{et} / cm s^{-1}	k_s / cm s^{-1}
amino-CNTs	0.36	16.0	6.3×10^{-7}	0.24	1.3×10^{-7}	2.8×10^{-8}
PBA-amino-CNTs	0.42	21.7	1.3×10^{-6}	0.32	2.5×10^{-6}	2.9×10^{-8}
PBA-amino-CNTs-Gr	0.45	22.1	2.5×10^{-6}	0.33	4.6×10^{-6}	9.3×10^{-8}

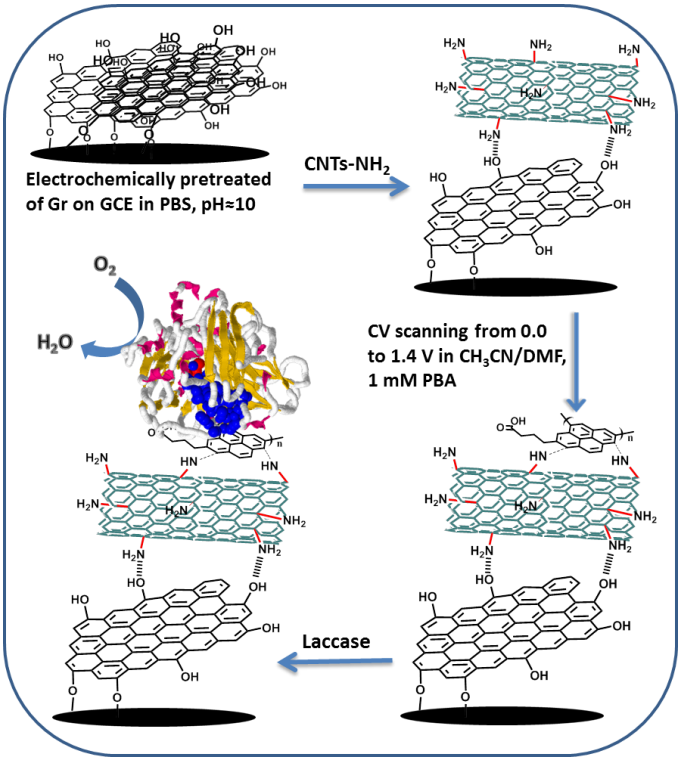

Scheme 1

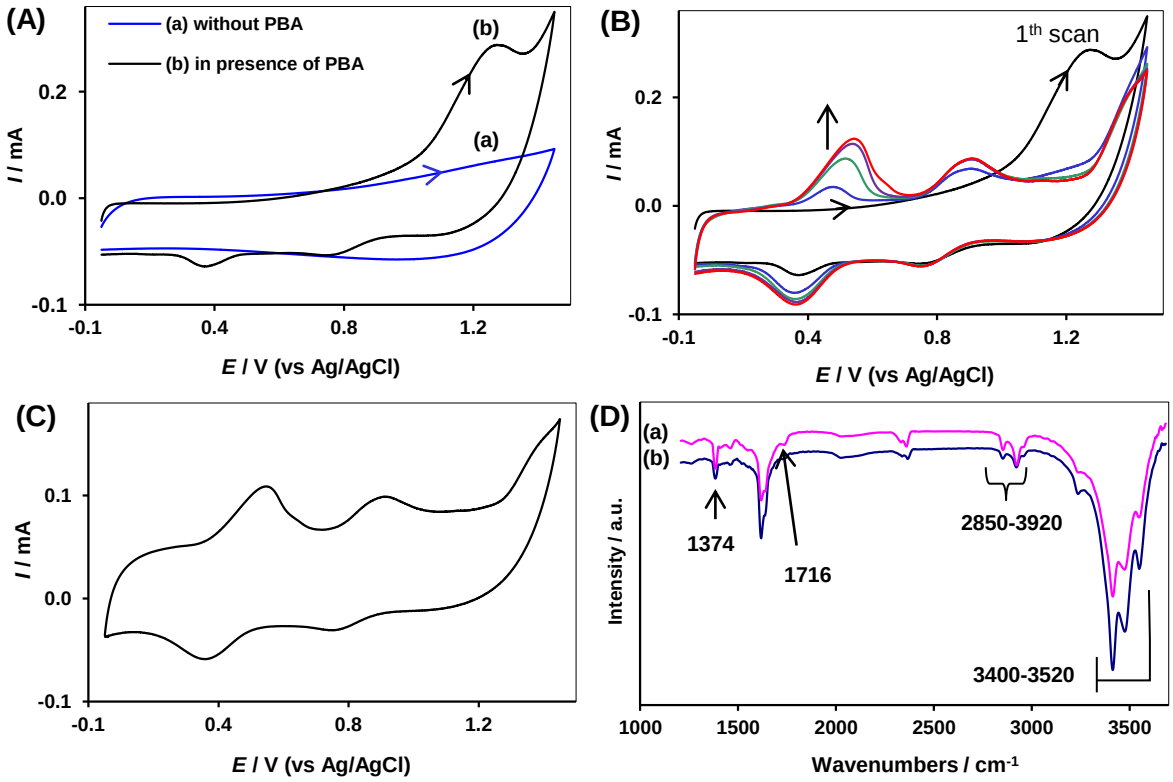

Figure 1

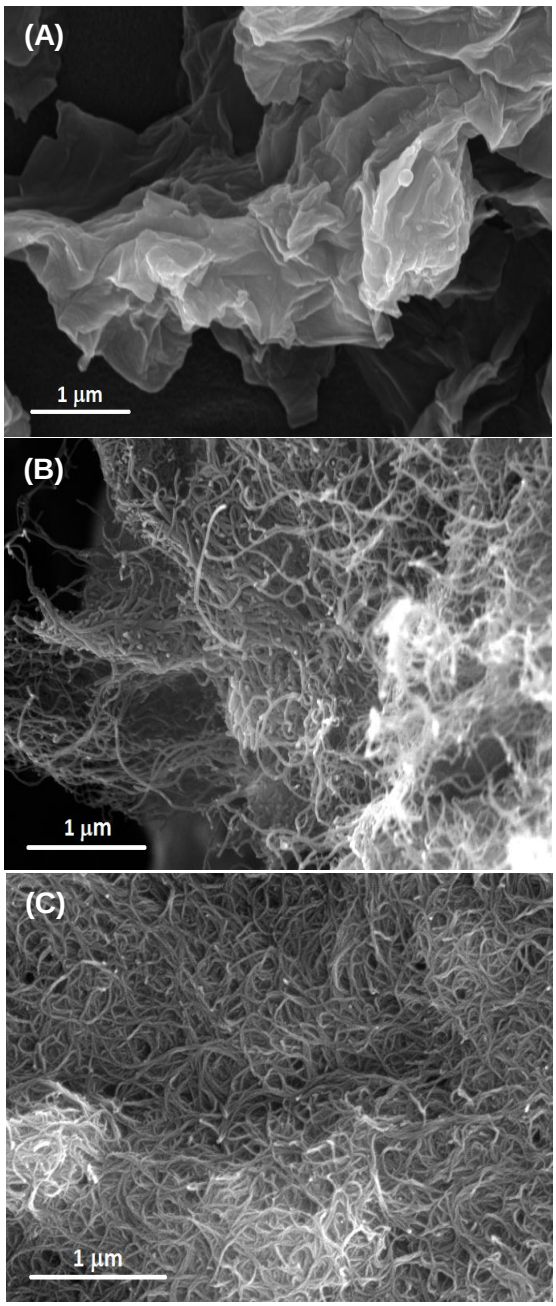

Figure 2

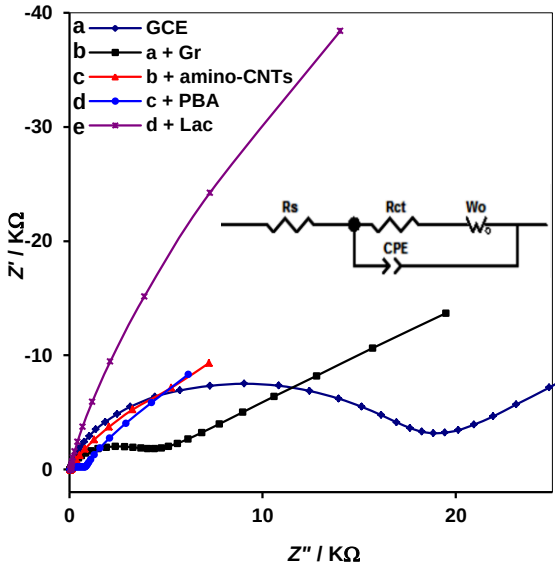

Figure 3

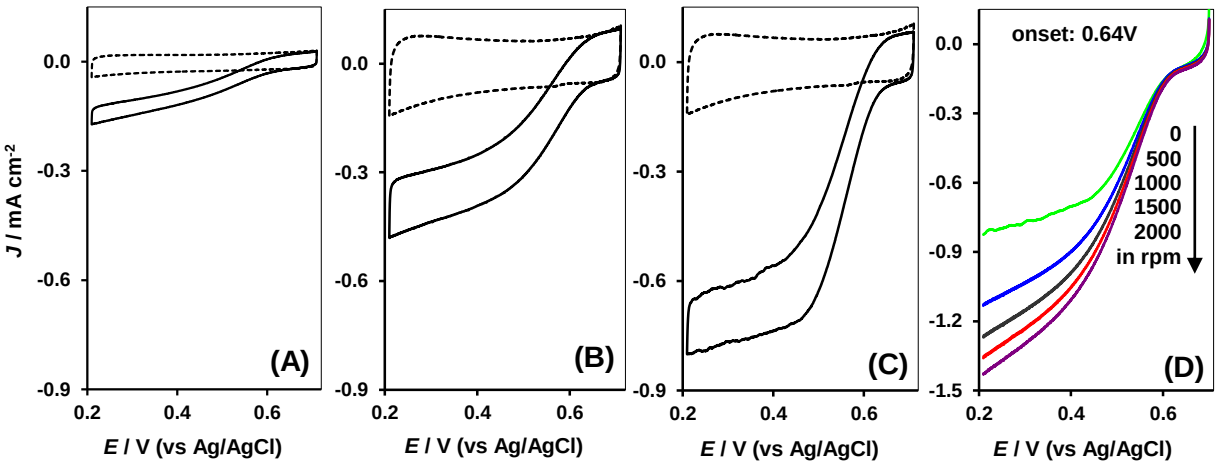

Figure 4

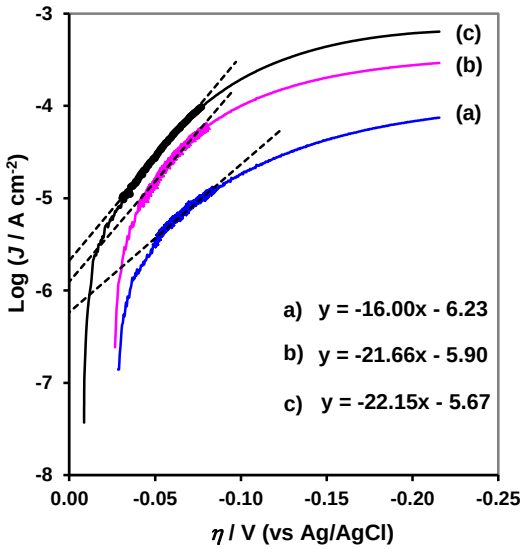

Figure 5

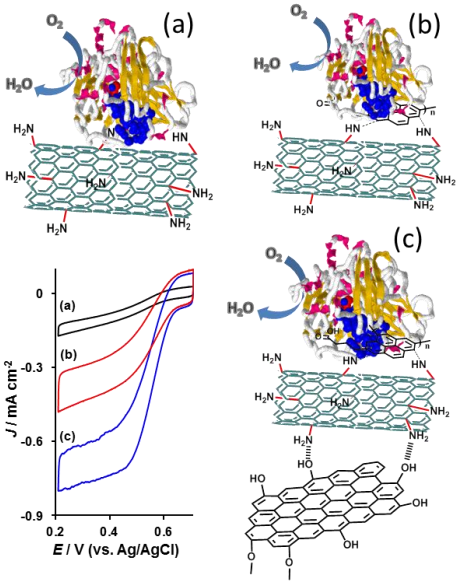

Graphical abstract

Graphical Abstract

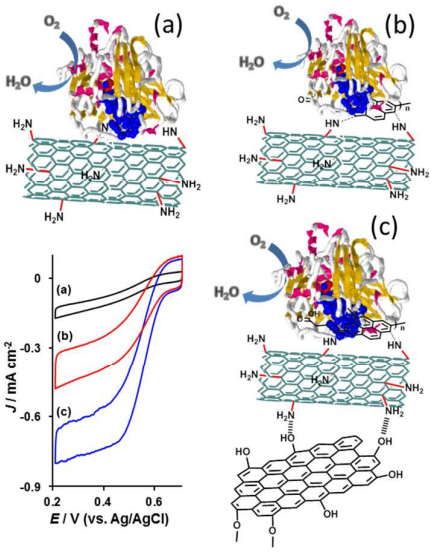

The amino-CNTs conjugated graphene functionalized with electropolymerized pyrene film used as novel hydrophobic platform for immobilization of LC and improving its electrocatalytic activity toward ORR .